

Spontaneous Synchronization in Cellular Circadian Clocks

Yuelong Li

December 2022

Abstract

In a previous paper, Wang and Peskin have provided a mathematical theory explaining the emergence of circadian rhythms from the interactions between molecules inside a single cell. In this paper, I am interested in the *emergent behavior* and *spontaneous synchronization* of the cellular clocks within a large number of *interacting* cells. In **section 3**, I generalize the previous model into the multiple cell regime, where molecules are exchanged intracellularly through diffusion over a bloodstream. In **section 4**, I observe the dynamics of such systems through numerical simulations, and put forth an original theory for its collective dynamics, which is a closed set of equations except for a parameter dependence on σ_{pn} , the standard deviation in the number of nucleus inhibitory protein across cells. In **appendix A**, I then solve for the time evolution of σ_{pn} analytically with perturbation approximations, and show that it decays at around a rate of $e^{-\frac{1}{4}\epsilon t}$, where ϵ is the exchange factor.

Contents

1	Introduction	3
2	Single Cell Model	3
2.1	Protein Binding	4
2.2	Continuous time model	5
2.3	Simulation	7
2.4	Validation	7
3	Multi Cell Model	8
3.1	Multi-cell simulation	9
4	Mean Flow Theory	14
4.1	Behavior of m_s	15
4.2	Behavior of σ_{pn}^2	17
5	Conclusion	19
Appendices		20

A Behavior of σ_{pn}^2 continued	20
B Verification of theory	24

1 Introduction

Beyond the simple one direction transcription and translation flow, proteins translated by ribosome in the cytoplasm can be imported into the nucleus, and interact with the DNA, forming complex cellular dynamics. In a previous paper by Wang and Peskin [1], a four species model was put forth describing the cellular dynamics governing circadian rhythms through the formation of non-linear phase oscillator.

In this paper I will generalize this dynamics into the regime of multiple interacting cells. Their cellular interaction is based on the assumption that some of the molecules governing the circadian cycle will diffuse into the blood stream, and some molecules in the blood stream will also diffuse into cell cytoplasm. The two diffusion process happen at different rates based on different concentrations of molecules inside and outside the cells, hence causing a kind of "exchange" which may give rise to synchronization. Then I will make attempts to simulate and theorize the emergent behaviors in an interacting system of cellular clocks such as synchronization, or collective damping.

2 Single Cell Model

In a single cell oscillator, our model consists of four species of molecules, which are respectively: mRNA in nucleus (m_n), mRNA in cytoplasm (m_c), protein in cytoplasm (p_c), and protein in the nucleus (p_n). mRNA are created through DNA transcription and enter into the cytoplasm through diffusion at a rate of γ_m (prb/hr), proteins are made in the cytoplasm and enter into the nucleus also through diffusion at a rate of γ_p (prb/hr). While concentration of mRNA molecules drive the transcription at a rate of β , proteins in the nucleus inhibits the transcription by binding to the DNA sites at a rate of ξ (prb/hr) and unbinding at a rate of η (prb/hr). Additionally, mRNA in the cytoplasm spontaneously degrade at a rate of δ_m and proteins in the nucleus at a rate of δ_p .

Reaction #	Name	Probability/Time	Result
1	Transcription	αP_0	$\#(m_n) \rightarrow \#(m_n) + 1$
2	Export	$\gamma_n m_n$	$\#(m_n) \rightarrow \#(m_n) - 1$
			$\#(m_c) \rightarrow \#(m_c) + 1$
3	Degradate n	$\gamma_c m_c$	$\#(m_c) \rightarrow \#(m_c) - 1$
4	Translation	βm_c	$\#(p_c) \rightarrow \#(p_c) + 1$
5	Import	$\gamma_p p_c$	$\#(p_c) \rightarrow \#(p_c) - 1$
			$\#(p_n) \rightarrow \#(p_n) + 1$
6	Degradate p	$\delta_p p_n$	$\#(p_n) \rightarrow \#(p_n) - 1$

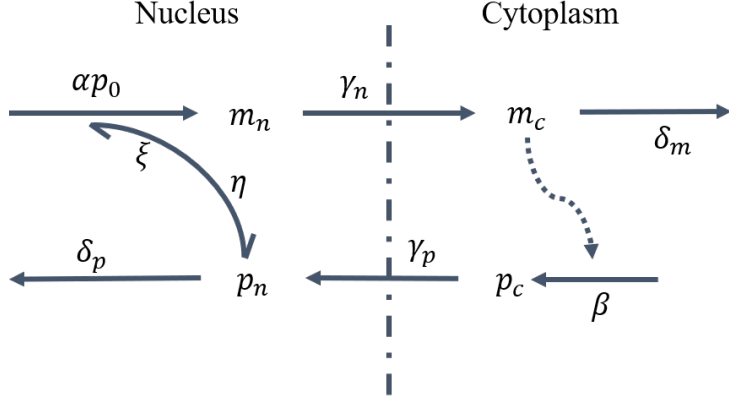


Figure 1: Molecular oscillator in a single cell

2.1 Protein Binding

m_p is only created when there are no inhibitory proteins bound to the DNA. To the probability per unit time that this process happens, we will also need the probability that there are no DNA bound to any of the DNA sites. $r \in \mathbb{Z}$ describes the number of sites there are on the DNA for inhibitory proteins to bind. Let k_1, k_2 be the macro rate constants corresponding to the micro rate constants ξ, η , with relations:

$$k_1[A][B] = \frac{d}{dt}[AB],$$

$$\xi \#(A) \#(B) = \frac{d}{dt} \#(AB).$$

By dividing both sides of the macro rate constant by the nucleus volume V , we get:

$$\xi = \frac{k_1}{V}.$$

Similarly:

$$k_2[AB] = \frac{d}{dt}[A] = \frac{d}{dt}[B],$$

$$\eta \#(AB) = \frac{d}{dt} \#(A) = \frac{d}{dt} \#(B).$$

$$\Rightarrow \eta = k_2.$$

So if we set $K = \frac{k_2}{k_1}$, then $\frac{\eta}{\xi} = KV$.

If we denote by P_l the probability that l sites are occupied, then αP_0 corresponds to the transcription rate. To find P_0 , we consider the fast probabilistic equilibrium between state P_l and P_{l+1} , satisfying:

$$\xi(r-l)(p_n-l)P_l = \eta(l+1)P_{l+1},$$

notice in this equation $r-l$ corresponds to the number of empty DNA sites for binding, p_n-l is the remaining number of proteins available for binding. On the right side, $l+1$ correspond to the number of bound DNA sites available for decomposition. Through manipulation of the relation, we can express P_l in terms of P_0 for all $l \in [\min(r, \#(p_n))]$. In our case we can

assume p_n to be large and there will always be proteins available for binding, so that l can run from 0 to r .

Then normalizing the total sum of probabilities to 1 yields (for large p_n):

$$P_0 = \frac{1}{\sum_{l=0}^r \binom{r}{l} \binom{p_n}{l} l! \left(\frac{\xi}{\eta}\right)^l} = \frac{1}{\sum_{l=0}^r \binom{r}{l} p_n^l \left(\frac{\xi}{\eta}\right)^l} = \frac{1}{(1 + p_n/KV)} = \frac{K}{(K + p_n/V)}. \quad (1)$$

2.2 Continuous time model

Now we have the value of P_0 in relation to p_n , we can write down the differential equations governing the molecular population. We will be using directly the molecule number instead of concentration in this paper, as they are more intuitive to work with, and cellular dynamics naturally involve small number of dynamics. But even though the molecule numbers are small, we will only be considering the molecule numbers under continuous change to simplify calculations. The previous paper [1] has provided thorough comparisons between the results obtained from stochastic and continuous models.

$$\begin{aligned} \frac{dm_n}{dt} &= \alpha \left(\frac{K}{K + \frac{p_n}{V}} \right)^r - \gamma_m m_n \\ \frac{dm_c}{dt} &= \gamma_m m_n - \delta_m m_c \\ \frac{dp_c}{dt} &= \beta m_c - \gamma_p p_c \\ \frac{dp_n}{dt} &= \gamma_p p_c - \delta_p p_n. \end{aligned}$$

The critical point of this system occurs when all derivatives go to 0. Then we obtain: $\alpha \left(\frac{K}{K + \frac{p_n}{V}} \right)^r = \gamma_m m_n = \delta_m m_c = \frac{\delta_m}{\beta} \gamma_p p_c = \frac{\delta_m}{\beta} \delta_p p_n$. Thus giving the equilibrium condition for p_n :

$$\begin{aligned} \alpha \left(\frac{K}{K + \frac{p_n}{V}} \right)^r &= \frac{\delta_m}{\beta} \delta_p p_n. \\ \Rightarrow \alpha \beta \left(\frac{K}{K + \frac{p_n}{V}} \right)^r &= \delta_m \delta_p p_n. \end{aligned} \quad (2)$$

Take the solution to this expression to be p_{n0} . Around the equilibrium point, we shall approximate the non-linear term in $\frac{dm_n}{dt}$ by:

$$\frac{\partial}{\partial p_n} \left(\alpha \left(\frac{K}{K + \frac{p_n}{V}} \right)^r \right) = -\frac{r \delta_p \delta_m}{\beta} \left(\frac{p_{n0}/V}{K + p_{n0}/V} \right) \equiv -a.$$

Then we obtain for $\tilde{x} = x - x_0$:

$$\begin{aligned} \frac{d\tilde{m}_n}{dt} &= a\tilde{p}_n - \gamma_m \tilde{m}_n \\ \frac{d\tilde{m}_c}{dt} &= \gamma_m \tilde{m}_n - \delta_m \tilde{m}_c \\ \frac{d\tilde{p}_c}{dt} &= \beta \tilde{m}_c - \gamma_p \tilde{p}_c \\ \frac{d\tilde{p}_n}{dt} &= \gamma_p \tilde{p}_c - \delta_p \tilde{p}_n. \end{aligned}$$

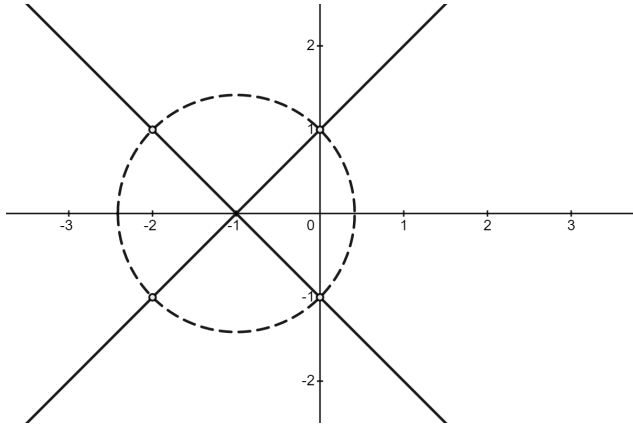


Figure 2: The possible values of λ/ν (solid lines) and the circle (dashed line) of radius $G^{\frac{1}{4}}$ that crosses it at the solutions of the characteristic (hollow points).

We shall let $\gamma_m = \delta_m = \gamma_p = \delta_p = \nu$. Then, characteristic of this linear expression satisfy:

$$\left(\frac{\lambda}{\nu} + 1\right)^4 = -\frac{a\beta}{\nu^2} = -r\nu^2 \left(\frac{p_{n0}/V}{K + p_{n0}/V}\right) \equiv -G.$$

For $(\frac{\lambda}{\nu} + 1)^4$ to equal a negative real number, $(\frac{\lambda}{\nu} + 1)$ must make 45 degree angles with the real axis in the complex plane. So for λ to have positive real part, it must hold that $|\frac{\lambda}{\nu} + 1| \geq \sqrt{1+1} = \sqrt{2}$, with $|G| = \left|(\frac{\lambda}{\nu} + 1)^4\right| \geq \sqrt{2}^4 \geq 4$. Then

$$G = r \left(\frac{p_{n0}/V}{K + p_{n0}/V}\right) \geq 4.$$

Because $\frac{p_n/V}{K+p_n/V} < 1$, we obtain $r > 4$. We shall take $r = 5$. Additionally, in the special case that $G = 4$, $(\frac{\lambda}{\nu} + 1)$ solves exactly to be $\lambda = i\nu$. This implies the oscillation cycle will a relatively constant amplitude, with an angular frequency of ν .

Because we want oscillation of 24 hours corresponding to the regular circadian rhythm, we shall take $\nu = \frac{2\pi}{24}$. On the other hand, due to the existence of non-linear terms in the actual differential equation, the solution are not perfect ellipsoids around the equilibrium points, and setting $\nu = \frac{2\pi}{22}$ gives a oscillator period of 24 hours, as we will see in the simulations. Now with $G = 4$, we may solve for K , in terms of p_{n0} :

$$K = \left(\frac{r}{4} - 1\right) p_n^0 / V.$$

Additionally, we take $\beta = 10\text{h}^{-1}$ from the previous paper and $V = 0.5(\text{pL})$ as a small arbitrary number to yield a reasonable value for α . With p_n^0 (the equilibrium point) given, we may solve for a value of α based on expression (2):

$$\alpha = \frac{\delta_m \delta_p p_n^0}{\beta} \left(\frac{K + p_n^0/V}{K}\right)^r.$$

We take $p_{n0} = 500$, so that the oscillation will always leave a large enough p_n for expression (1) to hold.

2.3 Simulation

With initialization conditions $m_n^0 = 10.9$, $m_c^0 = 1.88$, $p_n^0 = 500$, $p_c^0 = 250$ (these are initial values, not critical point values), and the following parameter initialization:

```

nu = 2*math.pi/22
gm = nu
dm = nu
gp = nu
dp = nu
r = 5
b = 10
V=0.1
pn0 = 500
K=(r/4-1)*pn0*V+1 #K = 63.5
a=dm*dp*pn0*((K+pn0/V)/K)**r/b #alpha => a = 5374068

```

we use the `scipy.integrate.solve_ivp` package [2] to obtain the following result (see figure 3).

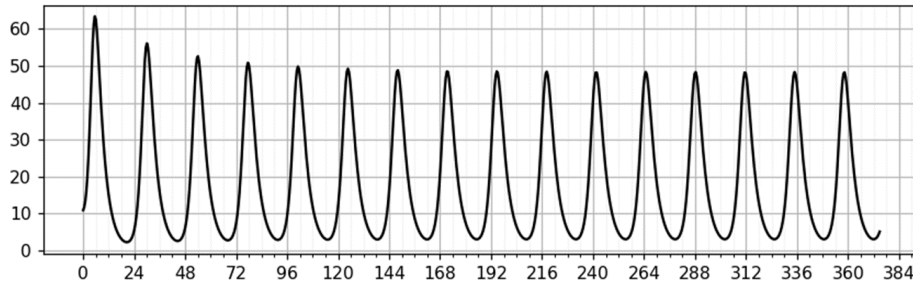


Figure 3: Molecular count for m_n versus time (in hours elapsed) for initial conditions given, which can be seen to stabilize into a fixed orbit.

The `scipy.integrate.solve_ivp` method by default uses the RK5(4) integration scheme, which is essentially a 5-th order Runge-Kutta integrator. As opposed to explicit methods like the classic RK4, the RK5(4) integrator is an embedded method, which produce an estimate of the local error in each step, and one can then use it to **adapt** the step size h and limit the error. The specific RK5(4) method this package implements is Dormand-Prince [3]. The relative tolerance is set to be 10^{-15} , so that in each step, the error $y_{n+1} - \Phi^{t_n, t_{n+1}} y_n$ cannot exceed $10^{-15} y_n$.

2.4 Validation

We plot the total number of proteins $p = p_n + p_c$ and take its derivative. We expect to see $\frac{dp}{dt} = \beta m_c - \delta_p p_n$. The expected rate of change of p_n and its actual rate of change match when integrator precision is set to 10^{-35} .

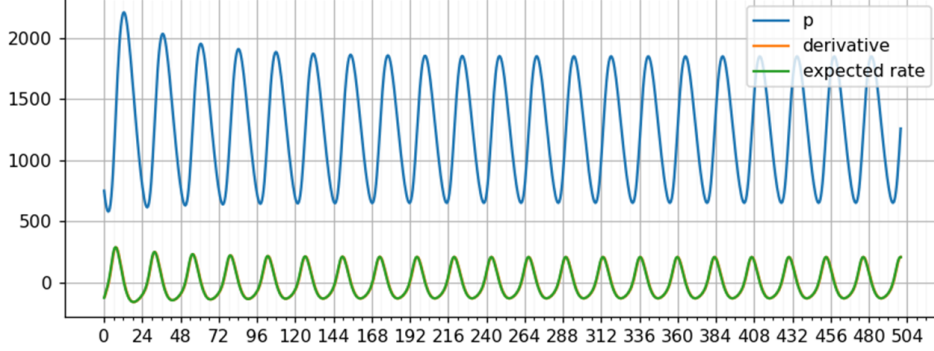


Figure 4: Total number of proteins (blue) and its derivative (orange, covered) vs time (hrs), which matches the expected rate of change (green).

3 Multi Cell Model

Now we introduce the augmented model including multiple cells and their interactions.

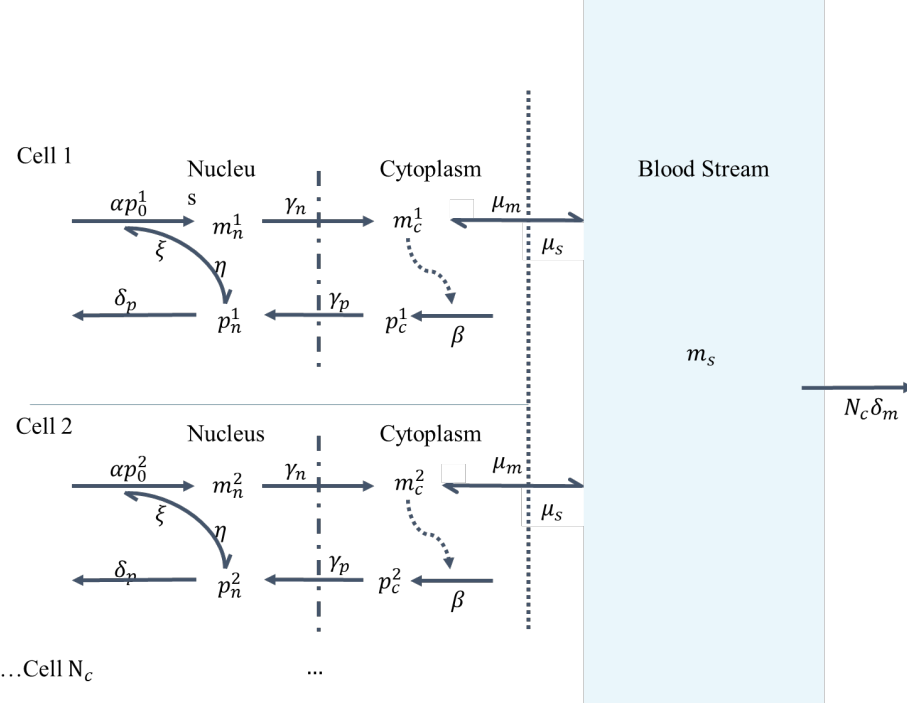


Figure 5: The molecular flow with additional parameters N_c : cell count, m_s : blood mRNA level, μ_m : membrane diffusion, μ_s : membrane infusion

In the multi-cell model, we attach all cells to a blood stream, and assume that cytoplasm mRNA m_c can travel from membrane into the blood stream or vice versa through diffusion. The two micro rate constants are μ_m and μ_s respectively. The model essentially considers all cells to be connect to a single vertex of blood stream, forming a star shape in their connection graph. This is valid because the production rate of mRNA is slow (on the scale of hours)

Reaction #	Name	Probability/Time	Result
1	Transcription	αp_0^i	$\#(m_n^i) \rightarrow \#(m_n^i) + 1$
2	Export	$\gamma_n m_n^i$	$\#(m_n^i) \rightarrow \#(m_n^i) - 1$
			$\#(m_c^i) \rightarrow \#(m_c^i) + 1$
3	Diffusion	$\mu_c m_c^i$	$\#(m_c^i) \rightarrow \#(m_c^i) - 1$
			$\#(m_s) \rightarrow \#(m_s) + 1$
4	Translation	βm_c^i	$\#(p_c^i) \rightarrow \#(p_c^i) + 1$
5	Import	$\gamma_p p_c^i$	$\#(p_c^i) \rightarrow \#(p_c^i) - 1$
			$\#(p_n^i) \rightarrow \#(p_n^i) + 1$
6	Degradate p	$\delta_p p_n^i$	$\#(p_n^i) \rightarrow \#(p_n^i) - 1$
7	Infusion	$\mu_s m_s$	$\#(m_c^i) \rightarrow \#(m_c^i) + 1$
			$\#(m_s) \rightarrow \#(m_s) - 1$
8	Degradate n	$N_c \delta_m m_s$	$\#(m_s) \rightarrow \#(m_s) - 1$

compared to the blood circulation rate, so it is not necessary to consider their locality in the blood stream.

We will keep all the previously specified constant with the same values. Additionally, cells no longer degrade mRNA molecules inside the cytoplasm, but instead diffuse them into the blood stream, where they are degraded at a rate of $N_c \delta_m m_s$. Note that the original constant δ_m is scaled by a factor of N_c , as there are N_c cells exporting mRNA molecules. To account for cellular exchange, we introduce parameter ϵ called the exchange rate, and let $\mu_n = \epsilon + \delta_m$, $\mu_p = \epsilon$. This way if synchronization is reached, the additional export of ϵm_c should cancel out the import of ϵm_s , leaving equivalently a degradation rate of $\delta_m m_c$. This way the individual cells will keep their dynamics discussed in section 2 when synchronized, and hence the circadian period of 24 hours. The new differential equations governing the cellular dynamics are:

$$\begin{aligned} \frac{dm_n^i}{dt} &= \alpha \left(\frac{K}{K + \frac{p_n^i}{V}} \right)^r - \gamma_m m_n^i \\ \frac{dm_c^i}{dt} &= \gamma_m m_n^i - \mu_m m_c^i + \mu_s m_s \\ \frac{dp_c^i}{dt} &= \beta m_c^i - \gamma_p p_c^i \\ \frac{dp_n^i}{dt} &= \gamma_p p_c^i - \delta_p p_n^i \\ \frac{dm_s}{dt} &= \sum_{i=1}^{N_c} \mu_c m_c^i - N_c \mu_s m_s - N_c \delta_m m_s \end{aligned}$$

Keep previous parameters unchanged: $\alpha, \beta, K, V, \gamma_m, \delta_m, \gamma_p, \delta_p$. Additional parameters, $\mu_c = \delta_m + \epsilon$, $\mu_s = \epsilon$, where ϵ is the exchange rate.

3.1 Multi-cell simulation

To know the starting state of each cells, we sample their molecule counts from a phase instant from the stabilized solutions obtained for a single cell. To sample a circadian cycle, we start at $t > 240$ and find t corresponding to the first and second minima of m_n concentration.

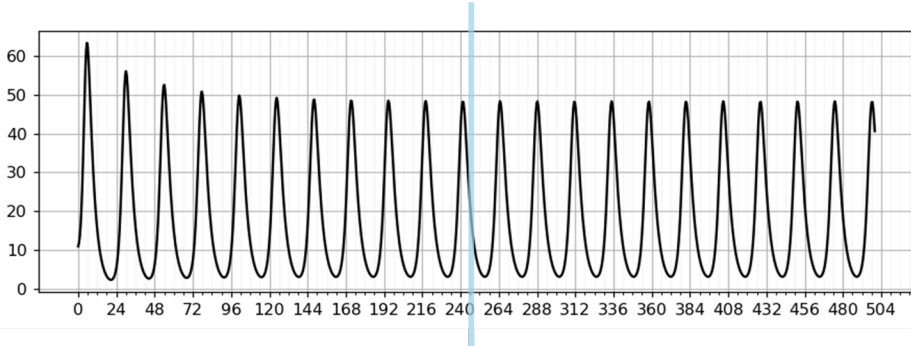


Figure 6: m_n vs t . We sample a single circadian cycle for $t > 240$, where the orbits have stabilized

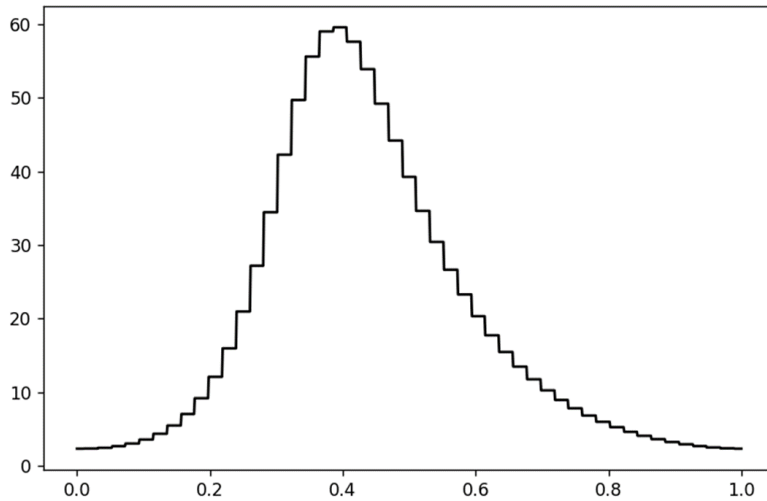
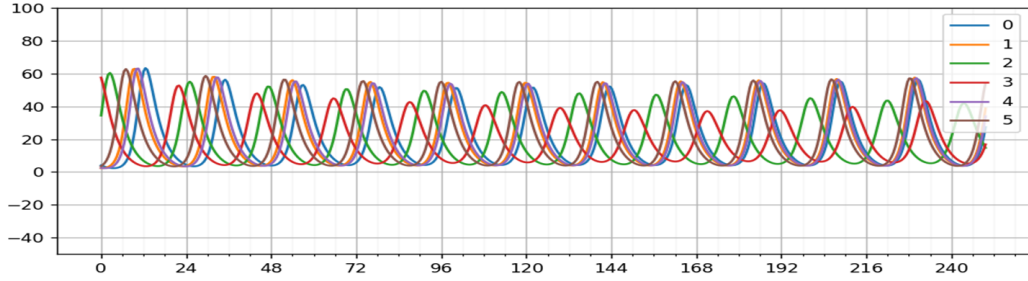


Figure 7: m_n v.s. t sampled over a period of dynamic equilibrium

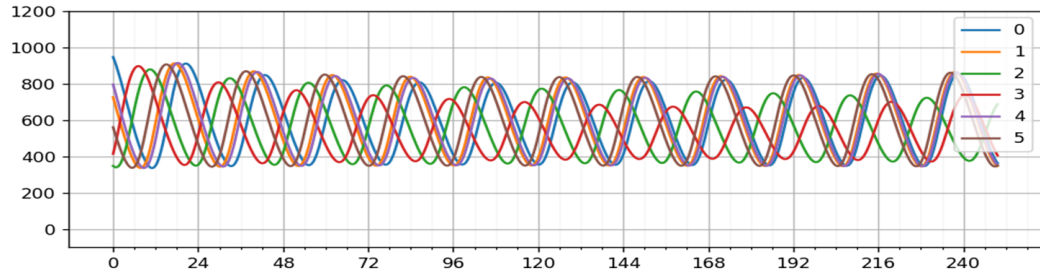
We then take the solution orbit $\mathbf{S} : [0, 2\pi] \rightarrow \mathbf{R}^4$ between these two timestamps as a single cycle, rescaled to $\phi \in [0, 2\pi]$. Next we randomize a list of $\{\phi_i\}$ from the uniform distribution between $[0, 2\pi]$. The initial conditions of each cells correspond to $\mathbf{S}(\phi_i)$.

For a 5 cell system, with $\epsilon = 2/22$, we obtain the result in **figure 8**. It can be observed that although slowly, the cellular concentrations are entering into phase coherence. After $t > 500$, the cellular phases are mostly synchronized. The blood mRNA of this 5 cell system are as shown in **figure 9**, where we can see that oscillation amplitude of m_s rises as the system enters into synchronization.

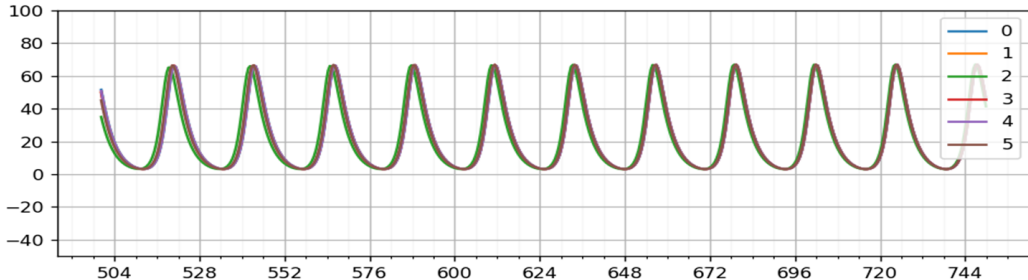
We continue the simulation to a 100 cell system, with $\epsilon = 1/11$, $\mu_s = \epsilon$, $\mu_c = \delta_m + \epsilon$, $\nu = \frac{2\pi}{11}$. The resultant orbits between $t = 0$ and $t = 250$ are shown in **figure 11**. We also compare m_s to m_c^i in **figure 10**, where m_s seems to oscillate within the phase space volume occupied by m_c^i .



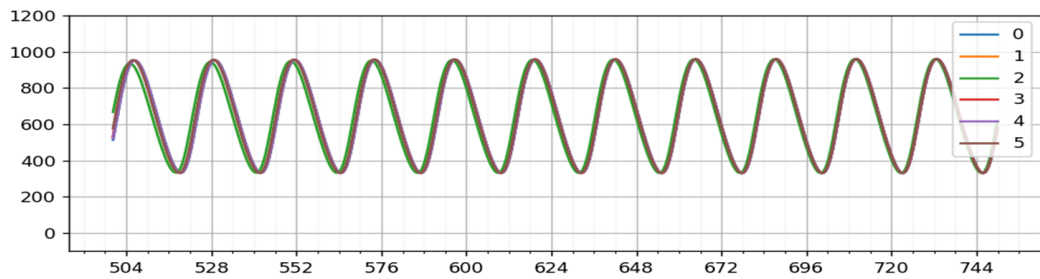
(a) m_n^i v.s. t , time between 0 and 250



(b) p_n^i v.s. t , time between 0 and 250

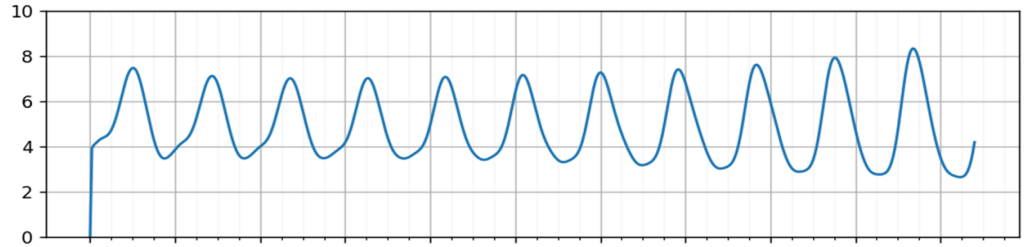


(c) m_n^i v.s. t , time between 500 and 750

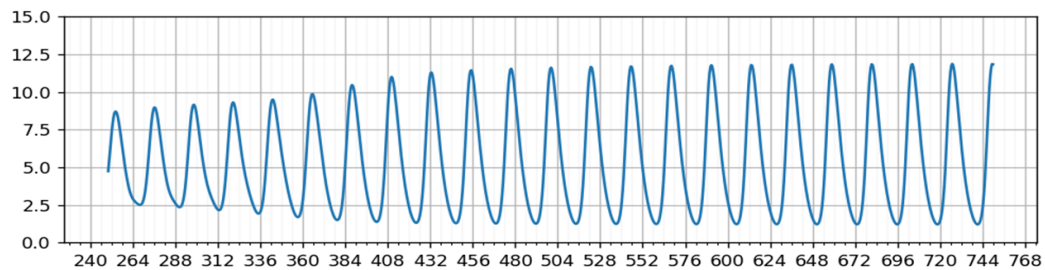


(d) p_n^i v.s. t , time between 500 and 750

Figure 8: Simulation result - 5 cells, $\epsilon = 2/22$, $\mu_c = \delta_m + \epsilon$, $\mu_s = 1 \neq \epsilon$.

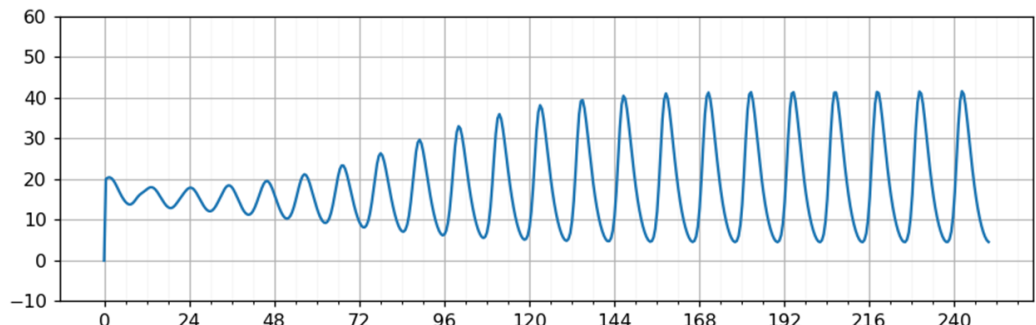


(a) m_s v.s. t , time between 0 and 250

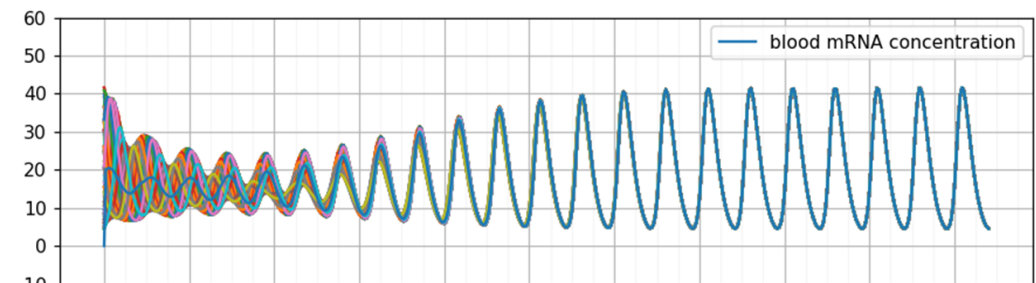


(b) m_s v.s. t , time between 250 and 750

Figure 9: Simulation result - 5 cells, $\epsilon = 2/22$, $\mu_c = \delta_m + \epsilon$, $\mu_s = 1 \neq \epsilon$.

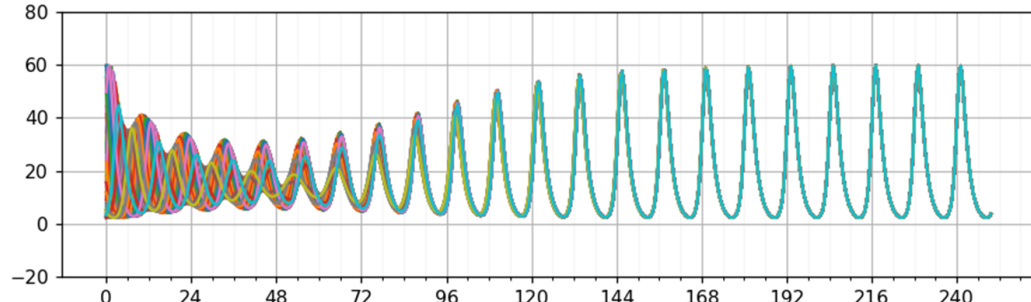


(a) m_s v.s. t

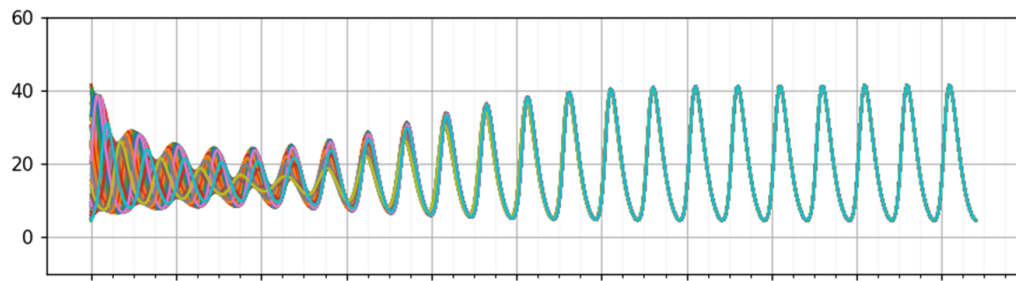


(b) m_s v.s. m_c^i

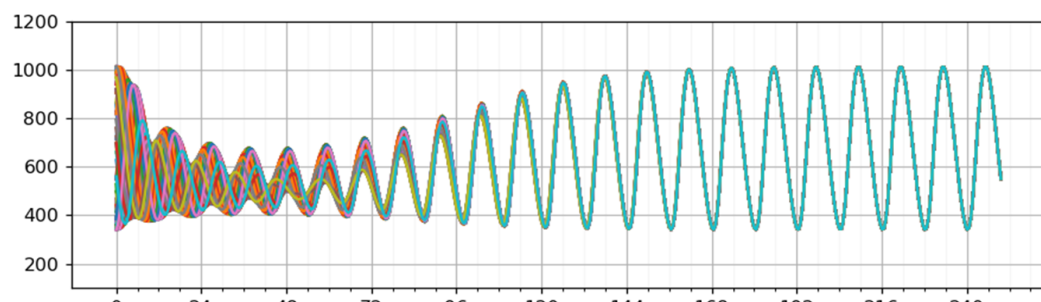
Figure 10: m_s comparison - 100 cells, $\epsilon = 2/22$, $\mu_c = \delta_m + \epsilon$, $\mu_s = 1 \neq \epsilon$.



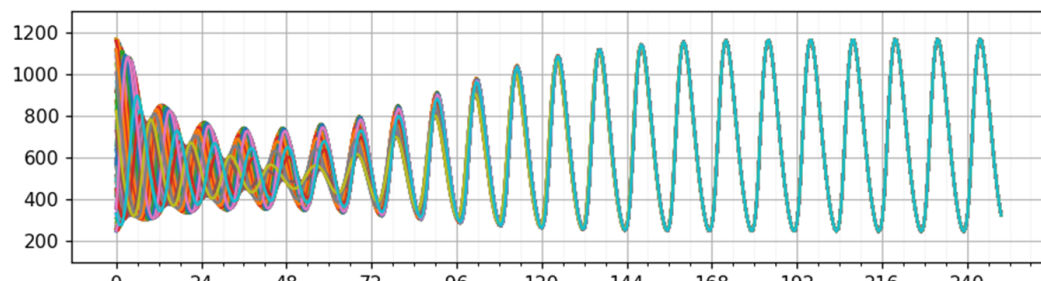
(a) m_n^i v.s. t



(b) m_c^i v.s. t



(c) p_n^i v.s. t



(d) p_c^i v.s. t

Figure 11: Simulation result - 100 cells, $\epsilon = 1/11$, $\mu_c = \delta_m + \epsilon$, $\mu_s = \epsilon$, $\nu = 2\pi/11$.

4 Mean Flow Theory

We want to explore in this section possible ways to explain and predict the emerging patterns such as synchronization and collective damping in the cellular system. The original equations of the system are:

$$\begin{aligned}\frac{dm_n^i}{dt} &= \alpha \left(\frac{K}{K + \frac{p_n^i}{V}} \right)^r - \gamma_m m_n^i \\ \frac{dm_c^i}{dt} &= \gamma_m m_n^i - \mu_m m_c^i + \mu_s m_s \\ \frac{dp_c^i}{dt} &= \beta m_c^i - \gamma_p p_c^i \\ \frac{dp_n^i}{dt} &= \gamma_p p_c^i - \delta_p p_n^i \\ \frac{dm_s}{dt} &= \sum_{i=1}^{N_c} \mu_c m_c^i - N_c \mu_s m_s - N_c \delta_m m_s\end{aligned}$$

which involves $4N_c + 1$ terms. For $N_c \gg 1$ solving it directly would be difficult. Inspired by mean-field theory in physics, we seek to reduce it to a set of 5 equations by taking their averages for $i \in [N_c]$. Then $x_i \rightarrow \langle x \rangle$ for all the dynamic variables. The summation term in $\frac{dm_s}{dt}$ is already averaging over m_c . So we obtain:

$$\begin{aligned}\frac{d \langle m_n \rangle}{dt} &= \frac{1}{N_c} \sum_{i=1}^{N_c} \alpha \left(\frac{K}{K + \frac{p_n^i}{V}} \right)^r - \gamma_m \langle m_n \rangle \\ \frac{d \langle m_c \rangle}{dt} &= \gamma_m \langle m_n \rangle - \mu_m \langle m_c \rangle + \mu_s m_s \\ \frac{d \langle p_c \rangle}{dt} &= \beta \langle m_c \rangle - \gamma_p \langle p_c \rangle \\ \frac{d \langle p_n \rangle}{dt} &= \gamma_p \langle p_c \rangle - \delta_p \langle p_n \rangle \\ \frac{d \langle m_s \rangle}{dt} &= N_c \mu_c \langle m_c \rangle - N_c \mu_s m_s - N_c \delta_m m_s.\end{aligned}$$

Unfortunately p_n^i in the first expression cannot be reduced due to non-linearity. However, we can take Taylor-expansion of each $\left(\frac{K}{K + \frac{p_n^i}{V}} \right)^r$ around $\langle p_n \rangle$. Then:

$$\begin{aligned}\frac{1}{N_c} \sum_{i=1}^{N_c} \alpha \left(\frac{K}{K + \frac{p_n^i}{V}} \right)^r &= \alpha \left(\frac{K}{K + \frac{\langle p_n \rangle}{V}} \right)^r + \frac{\alpha}{N_c} \frac{\partial}{\partial p_n} \left(\left(\frac{K}{K + \frac{p_n^i}{V}} \right)^r \right) \sum_{i=1}^{N_c} (p_n^i - \langle p_n \rangle) \\ &\quad + \frac{\alpha}{N_c} \frac{\partial^2}{\partial p_n^2} \left(\left(\frac{K}{K + \frac{p_n^i}{V}} \right)^r \right) \sum_{i=1}^{N_c} \frac{(p_n^i - \langle p_n \rangle)^2}{2} + \dots \\ &= \alpha \left(\frac{K}{K + \frac{\langle p_n \rangle}{V}} \right)^r + \frac{\alpha r(r+1)}{2K^2 V^2} \left(\frac{K}{K + \langle p_n \rangle / V} \right)^{(r+2)} \sigma_{pn}^2.\end{aligned}$$

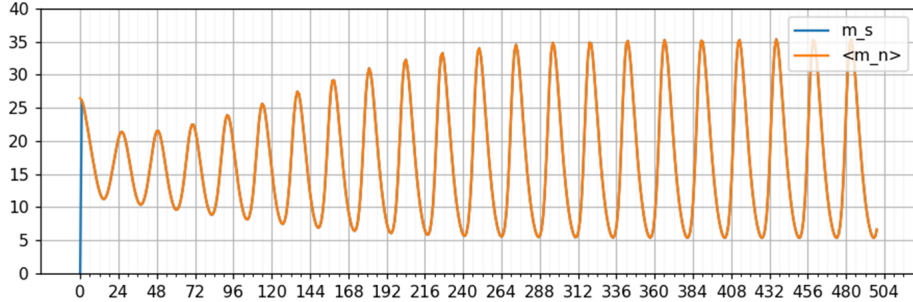


Figure 12: m_s vs t (blue) and $\langle m_c \rangle$ vs t (orange) with $N_c = 100$, $\nu = \frac{2\pi}{22}$, $\epsilon = \frac{2}{22}$

Plugging back we get:

$$\begin{aligned} \frac{d \langle m_n \rangle}{dt} &= \alpha \left(\frac{K}{K + \langle p_n \rangle / V} \right)^r + \frac{\alpha r(r+1)}{2K^2 V^2} \left(\frac{K}{K + \langle p_n \rangle / V} \right)^{(r+2)} \sigma_{pn}^2 - \gamma_m \langle m_n \rangle \\ \frac{d \langle m_c \rangle}{dt} &= \gamma_m \langle m_n \rangle - \mu_m \langle m_c \rangle + \mu_s m_s \\ \frac{d \langle p_c \rangle}{dt} &= \beta \langle m_c \rangle - \gamma_p \langle p_c \rangle \\ \frac{d \langle p_n \rangle}{dt} &= \gamma_p \langle p_c \rangle - \delta_p \langle p_n \rangle \\ \frac{d \langle m_s \rangle}{dt} &= N_c \mu_c \langle m_c \rangle - N_c \mu_s m_s - N_c \delta_m m_s. \end{aligned}$$

4.1 Behavior of m_s

We have hopes of further reducing this equation set by considering the last equation. Take $\mu_c = \epsilon + \delta_m$, $\mu_s = \epsilon$, then:

$$\frac{dm_s}{dt} = N_c(\epsilon + \delta_m) \langle m_c \rangle - N_c \epsilon m_s - N_c \delta_m m_s = N_c(\epsilon + \delta_m)(\langle m_c \rangle - m_s)$$

For $N_c \gg 1$, $\langle m_c \rangle - m_s \sim O(\langle m_c \rangle)$, $\frac{dm_s}{dt} \sim N_c O(\nu \langle m_c \rangle) \gg O(\nu \langle m_c \rangle) \sim \frac{d \langle m_c \rangle}{dt}$. So $\frac{d \langle m_c \rangle}{dt}$ is adiabatic compared to $\frac{dm_s}{dt}$ and:

$$\frac{d(m_s - \langle m_c \rangle)}{dt} \approx \frac{dm_s}{dt} = N_c(\epsilon + \delta_m)(\langle m_c \rangle - m_s).$$

Then solving with respect to $(m_s - \langle m_c \rangle)$, we get $m_s - \langle m_c \rangle = (m_s^0 - \langle m_c^0 \rangle) e^{-N_c(\epsilon + \delta_m)t}$. So for $t > 0$, we quickly have

$$m_s - \langle m_c \rangle \ll (m_s^0 - \langle m_c^0 \rangle) \Rightarrow m_s = \langle m_c \rangle.$$

In **figure 12**, we can see m_s quickly converging to $\langle m_c \rangle$ within an hour after the simulation starts.

Plugging this result back gives:

$$\begin{aligned}
\frac{d \langle m_n \rangle}{dt} &= \alpha \left(\frac{K}{K + \langle p_n \rangle / V} \right)^r + \frac{\alpha r(r+1)}{2K^2V^2} \left(\frac{K}{K + \langle p_n \rangle / V} \right)^{(r+2)} \sigma_{pn}^2 - \gamma_m \langle m_n \rangle \\
\frac{d \langle m_c \rangle}{dt} &= \gamma_m \langle m_n \rangle - \mu_m \langle m_c \rangle + \mu_s \langle m_c \rangle \\
\frac{d \langle p_c \rangle}{dt} &= \beta \langle m_c \rangle - \gamma_p \langle p_c \rangle \\
\frac{d \langle p_n \rangle}{dt} &= \gamma_p \langle p_c \rangle - \delta_p \langle p_n \rangle
\end{aligned}$$

Notice that this is just the same equation of motion of a single cell, with an additional term that depends on the standard deviation of p_n^i , which is an **extra dynamic variable** describing the system state. When σ_{pn} goes to 0, **it is guaranteed that the mean dynamics differential equations converge to that of the cellular dynamics of a single cell and will behave collectively like one.**

For $\sigma_{pn}^2 \neq 0$, we have new critical point of p_n satisfying:

$$\alpha\beta \left(\frac{K}{K + \langle p_n \rangle / V} \right)^r \left(1 + \frac{\sigma_{pn}^2 r(r+1)}{2K^2V^2} \left(\frac{K}{K + \langle p_n \rangle / V} \right)^2 \right) = \delta_m \delta_p \langle p_n \rangle,$$

which yields critical point $\langle p_n \rangle_0 > p_{n0}$. For first order approximation of the non-linear terms in $\frac{d \langle m_n \rangle}{dt}$,

$$\begin{aligned}
&\frac{\partial}{\partial \langle p_n \rangle} \left(\alpha \left(\frac{K}{K + \langle p_n \rangle / V} \right)^r + \frac{\alpha r(r+1)}{2V^2K^2} \left(\frac{K}{K + \langle p_n \rangle / V} \right)^{(r-2)} \sigma_{pn}^2 \right) \\
&= -\frac{\alpha r}{KV} \left(\frac{K}{K + \langle p_n \rangle_0 / V} \right)^{r+1} - \frac{\alpha r(r+1)(r+2)\sigma_{pn}^2}{2V^3K^3} \left(\frac{K}{K + \langle p_n \rangle_0 / V} \right)^{r+2} \equiv -a_1
\end{aligned}$$

So

$$a_1 = a + \frac{\alpha r(r+1)(r+2)}{2V^3K^3} \left(\frac{K}{K + \langle p_n \rangle_0 / V} \right)^{r+2} \sigma_{pn}^2.$$

Note that $a_1 > a$. With the same linear perturbation around the equilibrium as given in section 2, we have for G :

$$G_1 = \frac{a_1 \beta}{\nu^2} > \frac{a \beta}{\nu^2} = G,$$

then eigenvalues of the mean system will have positive real parts instead of 0 for the single cell case. This implies instability and a growing amplitude of oscillation. We can also see that as σ_{pn}^2 decreases at the beginning, it brings the critical point of the oscillation downwards from the original increased value, and the orbit of $\langle S \rangle$ simultaneously draws downward, before the amplitude increases and stabilizes as σ_{pn} converges to 0.

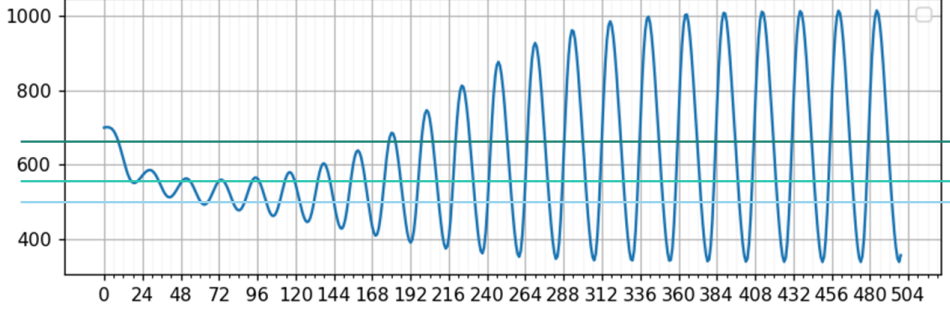


Figure 13: $\langle p_n \rangle$ vs t (blue), $N_c = 100, \nu = \frac{2\pi}{22}, \epsilon = \frac{2}{22}, V = 0.1$. Horizontal lines mark the decreasing critical values of $\langle p_n \rangle$.

4.2 Behavior of σ_{pn}^2

The above arguments justifies σ_{pn} as a measure of synchronization. Plugging in $m_s = \langle m_c \rangle$ into the single cell differential equations, we get:

$$\begin{aligned}\frac{dm_n^i}{dt} &= \alpha \left(\frac{K}{K + \frac{p_n^i}{V}} \right)^r - \gamma_m m_n^i \\ \frac{dm_c^i}{dt} &= \gamma_m m_n^i - \delta_m m_c^i + \epsilon(\langle m_c \rangle - m_c^i) \\ \frac{dp_c^i}{dt} &= \beta m_c^i - \gamma_p p_c^i \\ \frac{dp_n^i}{dt} &= \gamma_p p_c^i - \delta_p p_n^i,\end{aligned}$$

note that the term $\epsilon(\langle m_c \rangle - m_c^i)$ is driving the synchronization. As $\langle m_c \rangle - m_c^i$ goes to 0, the cellular dynamics of each individual cells stabilize to their original orbits.

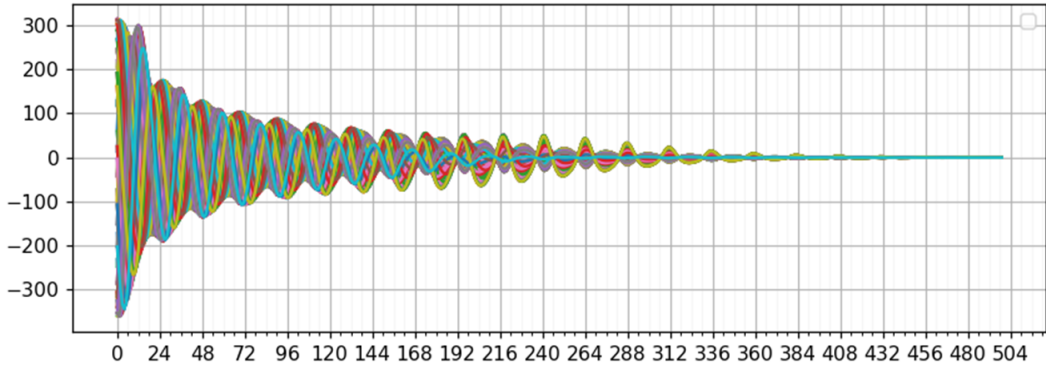


Figure 14: $p_n^i - \langle p_n \rangle$ vs t in an 100 cell simulation, with $\nu = \frac{2\pi}{22}, \epsilon = \frac{2}{22}, V = 0.1$

From the simulations we can observe that for a 100 cell system, the variance, namely $\sigma_{pn}^2 = \langle (p_n^i - \langle p_n \rangle)^2 \rangle$, drops exponentially and so does the standard deviation σ_{pn} . The

decay rate is initially determined to be 0.173ϵ via visual comparisons. This has worked for different choices of ν and ϵ (**figure 15, 16, 17**). Holistically, if we apply variation of constants to the second equation $\frac{dm_c^i}{dt} = \gamma_m m_n^i - \delta_m m_c^i + \epsilon(\langle m_c \rangle - m_c^i)$ alone, we shall obtain

$$m_c^i - \langle m_c \rangle \sim (m_c^{i0} - \langle m_c \rangle^0) e^{-\epsilon t},$$

with which we can estimate that

$$p_n^i - \langle p_n \rangle \sim (p_n^{i0} - \langle p_n \rangle^0) e^{-\epsilon t},$$

which gives that $\sigma_{pn} \sim \sigma_{pn}^0 e^{-\epsilon t}$.

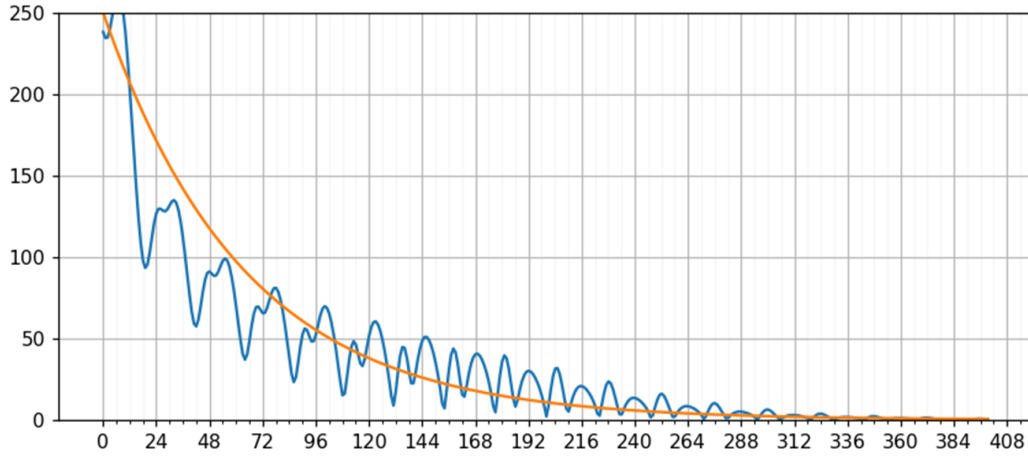


Figure 15: σ_{pn} vs t in 100 cell simulation, with $\nu = \frac{2\pi}{22}$, $\epsilon = \frac{2}{22}$, $V = 0.1$; $250e^{-0.173\epsilon t}$ (orange)

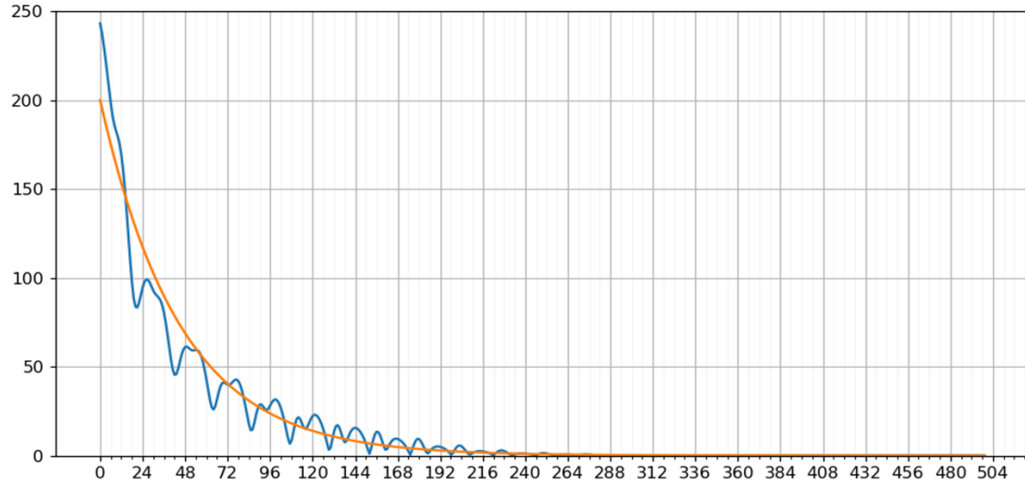


Figure 16: σ_{pn} vs t in 100 cell simulation (blue), with $\nu = \frac{2\pi}{22}$, $\epsilon = \frac{3}{20}$, $V = 0.1$; $250e^{-0.173\epsilon t}$ (orange)

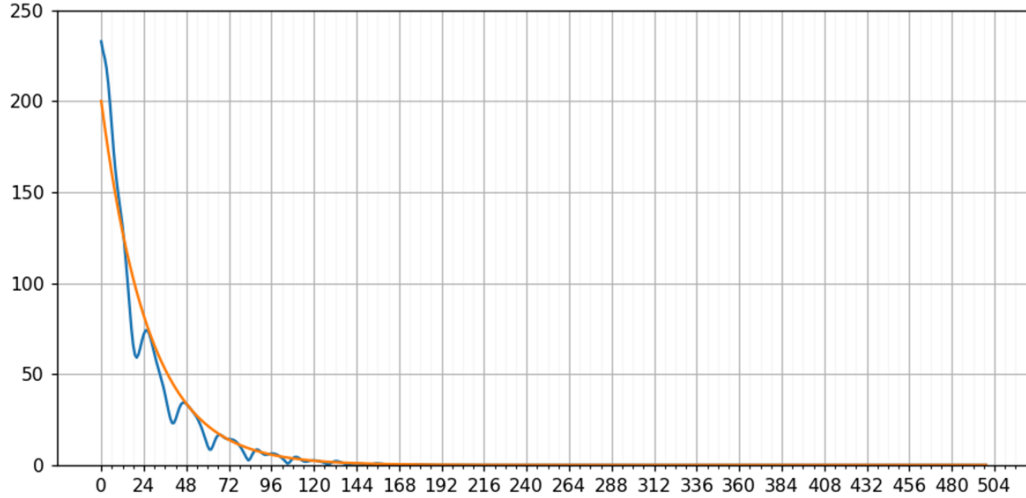


Figure 17: σ_{pn} vs t in 100 cell simulation (blue), with $\nu = \frac{2\pi}{22}$, $\epsilon = \frac{5}{20}$, $V = 0.1$; $250e^{-0.173\epsilon t}$ (orange)

In the appendix, I provide a complete variation of constants integration on the entire equation set, and obtain the more theoretically rigorous decay rate of $\frac{1}{4}\epsilon t$. The coefficient $\frac{1}{4} = 0.25$ is slightly larger than 0.173, and is experimentally confirmed to be a good lower-bound of the standard deviation, and tends to describe the decay more accurately as the cell number increases.

5 Conclusion

In this paper I have expanded the single cell to multiple cell model acting as an interactive system, by introducing a blood stream and an exchange rate ϵ that is relatively small compared to the other diffusion rates γ_m , γ_p , etc. Simulations of this system show strong trends toward synchronization for large number of interacting cells. I also re-expressed the $(4N+1)$ differential equations governing the multi cell system by a simpler set of 4 involving the mean quantities of the systems and an additional standard deviation term (spread) of cytoplasm concentrations of the protein species across cells. This allows one to make qualitative conclusions about the dynamics of the averages of the cellular quantities, and hence their collective behavior. I provided a theoretical argument for the values of σ_{pn} evolving through time, and determined it to decay by a factor of $e^{-0.25\epsilon t}$ for relatively small values of ϵ .

Appendices

A Behavior of σ_{pn}^2 continued

Starting again with the individual cell equations connected to a bloodstream,

$$\begin{aligned}\frac{dm_n^i}{dt} &= \alpha \left(\frac{K}{K + \frac{p_n^i}{V}} \right)^r - \gamma_m m_n^i \\ \frac{dm_c^i}{dt} &= \gamma_m m_n^i - (\delta_m + \epsilon) m_c^i + \epsilon \langle m_c \rangle \\ \frac{dp_c^i}{dt} &= \beta m_c^i - \gamma_p p_c^i \\ \frac{dp_n^i}{dt} &= \gamma_p p_c^i - \delta_p p_n^i,\end{aligned}$$

We denote the phase flow of the system by $S^i : \mathbb{R} \rightarrow \mathbb{R}^4$, $S^i = (m_n^i, m_c^i, p_c^i, p_n^i)$. The **first assumption** is that the term $\epsilon \langle m_c \rangle$ is a function of time that runs *independently* of S^i . This is because for large amount of cells, the fluctuations in one individual cell contributes to only a tiny amount of the mean dynamics, $\langle S \rangle$ can be thought of as an oscillator independent of each S^i . So the *homogeneous* part of the equation set reduces to be:

$$\begin{aligned}\frac{dm_n^i}{dt} &= \alpha \left(\frac{K}{K + \frac{p_n^i}{V}} \right)^r - \gamma_m m_n^i \\ \frac{dm_c^i}{dt} &= \gamma_m m_n^i - (\delta_m + \epsilon) m_c^i \\ \frac{dp_c^i}{dt} &= \beta m_c^i - \gamma_p p_c^i \\ \frac{dp_n^i}{dt} &= \gamma_p p_c^i - \delta_p p_n^i,\end{aligned}$$

The **second assumption** we make is that S^i oscillates in a vicinity to the critical point of the *homogeneous equation*, $S^0 = (m_n^0, m_c^0, p_c^0, p_n^0)$, as described in section 2.2 with the added term of ϵ , satisfying:

$$\alpha \left(\frac{K}{K + \frac{p_n^0}{V}} \right)^r = \gamma_m m_n^0 = (\delta_m + \epsilon) m_c^0 = \frac{\delta_m + \epsilon}{\beta} \gamma_p p_c^0 = \frac{\delta_m + \epsilon}{\beta} \delta_p p_n^0.$$

Then we can again express the non-linear term $\alpha \left(\frac{K}{K + \frac{p_n^i}{V}} \right)^r$ as its linear expansion $\alpha \left(\frac{K}{K + \frac{p_n^0}{V}} \right)^r - a(p_n^i - p_n^0)$. Again

$$a \equiv \frac{r \delta_p \delta_m}{\beta} \left(\frac{p_{n0}/V}{K + p_{n0}/V} \right).$$

Then replacing each variable in the equation by its displacement from the equilibrium, namely with $\tilde{S}^i = S^i - S^0$, we have (after cancellations):

$$\begin{aligned}\frac{d\tilde{m}_n^i}{dt} &\approx -a\tilde{p}_n^i - \gamma_m\tilde{m}_n^i \\ \frac{d\tilde{m}_c^i}{dt} &= \gamma_m\tilde{m}_n^i - (\delta_m + \epsilon)\tilde{m}_c^i + \epsilon \langle m_c \rangle \\ \frac{d\tilde{p}_c^i}{dt} &= \beta\tilde{m}_c^i - \gamma_p\tilde{p}_c^i \\ \frac{d\tilde{p}_n^i}{dt} &= \gamma_p\tilde{p}_c^i - \delta_p\tilde{p}_n^i.\end{aligned}$$

If we define projector matrix $P = \begin{pmatrix} 0 & 0 & 0 & 0 \\ 0 & 1 & 0 & 0 \\ 0 & 0 & 0 & 0 \\ 0 & 0 & 0 & 0 \end{pmatrix}$, then $P \langle S \rangle = \begin{pmatrix} 0 \\ \langle m_c \rangle \\ 0 \\ 0 \end{pmatrix}$.

We shall define matrix

$$A = \begin{pmatrix} -\gamma_m & 0 & 0 & -a \\ \gamma_m & -(\delta_m + \epsilon) & 0 & 0 \\ 0 & \beta & -\gamma_p & 0 \\ 0 & 0 & \gamma_p & -\delta_p \end{pmatrix} = A_0 - \epsilon P, \text{ where } A_0 = \begin{pmatrix} -\gamma_m & 0 & 0 & -a \\ \gamma_m & -\delta_m & 0 & 0 \\ 0 & \beta & -\gamma_p & 0 \\ 0 & 0 & \gamma_p & -\delta_p \end{pmatrix}$$

is the matrix governing the single cell orbits near its critical point (as discussed in section 2.2). Now we can rewrite the individual cell equations in the matrix form:

$$\frac{d}{dt}\tilde{S}^i = A\tilde{S}^i + \epsilon P \langle S \rangle.$$

To apply variation of constants, we first solve the homogeneous part:

$$\frac{d}{dt}\tilde{S}^i = A\tilde{S}^i \Rightarrow \tilde{S}^i = e^{At}C, \quad C \in \mathbb{R}^4.$$

Next we shall let C be a function of time, and plug this result back to obtain:

$$\frac{d}{dt}\tilde{S}^i = A\tilde{S}^i + e^{At}\frac{d}{dt}C = A\tilde{S}^i + \epsilon P \langle S \rangle,$$

so

$$e^{At}\frac{d}{dt}C = \epsilon P \langle S \rangle \Rightarrow C = \int e^{-At}\epsilon P \langle S \rangle dt.$$

Then we obtain the analytical result of \tilde{S}^i , noting $\langle S \rangle$ to be a function of time,

$$\tilde{S}^i = e^{At} \left(\int e^{-At}\epsilon P \langle S \rangle dt \right) = e^{At} \left(\int_{t_0}^t e^{-At}\epsilon P \langle S \rangle dt + \tilde{S}_0^i \right),$$

where $\tilde{S}_0^i \in \mathbb{R}^4$ is the initial state of the individual cell of index $i \in [N_c]$. Now to find variance $\langle (S - \langle S \rangle)^2 \rangle = \langle (\tilde{S} - \langle \tilde{S} \rangle)^2 \rangle$, we first notice

$$\begin{aligned}\tilde{S}^i - \langle \tilde{S} \rangle &= e^{At} \left(\int_{t_0}^t e^{-At} \epsilon P \langle S \rangle dt + \tilde{S}_0^i \right) - \left\langle e^{At} \left(\int_{t_0}^t e^{-At} \epsilon P \langle S \rangle dt + \tilde{S}_0^i \right) \right\rangle \\ &= e^{At} \int_{t_0}^t e^{-At} \epsilon P \langle S \rangle dt + e^{At} \tilde{S}_0^i - \left\langle e^{At} \int_{t_0}^t e^{-At} \epsilon P \langle S \rangle dt + e^{At} \tilde{S}_0^i \right\rangle \\ &= e^{At} \int_{t_0}^t e^{-At} \epsilon P \langle S \rangle dt - \left\langle e^{At} \int_{t_0}^t e^{-At} \epsilon P \langle S \rangle dt \right\rangle + e^{At} \tilde{S}_0^i - \left\langle e^{At} \tilde{S}_0^i \right\rangle \\ &= e^{At} \tilde{S}_0^i - e^{At} \langle \tilde{S}_0 \rangle \\ &= e^{At} \left(\tilde{S}_0^i - \langle \tilde{S}_0 \rangle \right).\end{aligned}$$

Reminding ourselves of how \tilde{S}_0^i were initialized as in section 3.1, we know that $S_0^i = \mathbf{S}(\phi_i)$, where \mathbf{S} runs over a period of the sampled orbit of the single cell system. Under the assumption of small perturbation, we can argue that $\mathbf{S}(\phi_i) = \text{Re}\{e^{j\phi_i} \tilde{\mathbf{S}}_0\} + \mathbf{S}^0$, where $\tilde{\mathbf{S}}_0$, to be differentiated from \tilde{S}_0 , is the *initial* phase of the sampled orbit of the single cell system, and \mathbf{S}^0 is the critical point of the single cell system. Then

$$\tilde{S}_0^i = S_0^i - S^0 = \text{Re}\{e^{j\phi_i} \tilde{\mathbf{S}}_0\} + \mathbf{S}^0 - S^0.$$

For small ϵ , the critical point of the single cell system and the critical point of the individual cell dynamics in a multi-cell system should roughly be the same, so

$$\tilde{S}_0^i = \text{Re}\{e^{j\phi_i} \tilde{\mathbf{S}}_0\} + \mathbf{S}^0 - S^0 = \text{Re}\{e^{j\phi_i} \tilde{\mathbf{S}}_0\} + O(\epsilon) = \text{Re}\{e^{j\phi_i} \tilde{\mathbf{S}}_0\}.$$

Then for large number of cells sampled uniformly over a period,

$$\langle \tilde{S}_0 \rangle = \int_0^{2\pi} \text{Re}\{e^{j\phi} \tilde{\mathbf{S}}_0\} d\phi / 2\pi = 0,$$

so

$$\tilde{S}^i - \langle \tilde{S} \rangle = e^{At} \left(\tilde{S}_0^i - \langle \tilde{S}_0 \rangle \right) = e^{At} \tilde{S}_0^i.$$

Going back to A , we shall seek for its eigenvalues, first noting that its eigenvalues satisfy the characteristic equation, for $\gamma_m = \delta_m = \gamma_p = \delta_p = \nu$:

$$(\nu + \lambda)^3(\nu + \epsilon + \lambda) + a\nu^3 = 0. \quad (3)$$

Now we know for the single cell system, the characteristic function corresponding to its matrix A_0 is:

$$(\nu + \lambda_0)^4 + a\nu^3 = 0, \quad (4)$$

denote solutions to this equation by λ_0 . Now since ϵ is small compared to ν by construction, we may also assume that λ deviates from λ_0 for a only small amount. If we consider $(\nu + \lambda)^3(\nu + \epsilon + \lambda)$ as a two variable function of λ and ϵ , equation 3 and 4 correspond to solutions

on the level set $(\nu + \lambda)^3(\nu + \epsilon + \lambda) = -a\nu^3$ for different values of ϵ . Let $\lambda = \lambda_0 + \delta\lambda$, $\epsilon = 0 + \delta\epsilon$, we have the constraint condition for a level set under variations:

$$\frac{\partial}{\partial \lambda} ((\nu + \lambda)^3(\nu + \epsilon + \lambda)) \delta\lambda + \frac{\partial}{\partial \epsilon} ((\nu + \lambda)^3(\nu + \epsilon + \lambda)) \delta\epsilon \Big|_{\epsilon=0, \lambda=\lambda_0} = 0.$$

This results in:

$$4(\nu + \lambda_0)^3 \delta\lambda + (\nu + \lambda_0)^3 \delta\epsilon = 0,$$

i.e.

$$\delta\lambda = -\frac{1}{4}\delta\epsilon.$$

Recall from section 2.2, two of the eigenvalues are $\lambda_0 = \pm i\nu$ by construction. Then $\lambda = \pm i\nu - \frac{1}{4}\delta\epsilon = \pm i\nu - \frac{1}{4}\epsilon$. The other two solutions of the eigenvalue already have large negative real parts of -2ν (see figure 2), and will forseeably damp out immediately on their own. Then

$$\tilde{S}^i - \langle \tilde{S} \rangle = e^{At} \tilde{S}_0^i = e^{(i\nu - \frac{1}{4}\epsilon)t} V_1(\phi_i) + e^{(-i\nu - \frac{1}{4}\epsilon)t} V_2(\phi_i) + e^{\lambda_3 t} V_3(\phi_i) + e^{\lambda_4 t} V_4(\phi_4),$$

where $V_k(\phi_i)$ are complex valued eigenvectors of A satisfying: $\tilde{S}_0^i = \sum_{k=1}^4 V_k(\phi_i)$. For $t > 0$, the last two terms involving V_3 and V_4 quickly disappears. Then for $t > 0$, we have, approximately,

$$\tilde{S}^i - \langle \tilde{S} \rangle = e^{At} \tilde{S}_0^i \approx e^{-\frac{1}{4}\epsilon t} \operatorname{Re} \{ e^{i\nu t} V_1(\phi_i) + e^{-i\nu t} V_2(\phi_i) \},$$

then under the assumption of uniform distribution of phase ϕ between $[0, 2\pi]$, we have:

$$\begin{aligned} \sigma^2 &= \langle (\tilde{S} - \langle \tilde{S} \rangle)^2 \rangle \\ &\approx \int_0^{2\pi} \left(e^{-\frac{1}{4}\epsilon t} \operatorname{Re} \{ e^{i\nu t} V_1(\phi) + e^{-i\nu t} V_2(\phi) \} \right)^2 d\phi / 2\pi \\ &= e^{-\frac{1}{8}\epsilon t} \int_0^{2\pi} (e^{i\nu t} V_1(\phi) + e^{-i\nu t} V_2(\phi))^2 d\phi / 2\pi \\ &= e^{-\frac{1}{8}t} \int_0^{2\pi} ({}^2 e^{2i\nu t} V_1(\phi)^2 + {}^2 e^{-2i\nu t} V_2(\phi)^2 + 2V_1 * V_2) d\phi / 2\pi \\ &= e^{-\frac{1}{8}t} \left(\frac{1}{\pi} \int_0^{2\pi} V_1(\phi) * V_2(\phi) d\phi + e^{2i\nu t} \frac{1}{2\pi} \int_0^{2\pi} V_1(\phi)^2 d\phi + e^{-2i\nu t} \frac{1}{2\pi} \int_0^{2\pi} V_2(\phi)^2 d\phi \right). \end{aligned}$$

This gives a constant amplitude

$$W \equiv \operatorname{Re} \left\{ \frac{1}{\pi} \int_0^{2\pi} V_1(\phi) * V_2(\phi) d\phi \right\} \quad (5)$$

and a fluctuating amplitude

$$\cos(2\nu t + \Phi_0) B \equiv \operatorname{Re} \left\{ e^{2i\nu t} \frac{1}{2\pi} \int_0^{2\pi} V_1(\phi)^2 d\phi + e^{-2i\nu t} \frac{1}{2\pi} \int_0^{2\pi} V_2(\phi)^2 d\phi \right\} \quad (6)$$

oscillating at the frequency of 2ν , where $\Phi_0 \in \mathbb{R}^4$ describe the initial phases of the orbits.

If $V_1(\phi)$ and $V_2(\phi)$ are also eigenvectors to the matrix A_0 , then we'd know they are conjugate pairs displaced by a phase of $\exp\{i\phi\}$ and $\exp\{-i\phi\}$ respectively from some initial eigenstates $U_1 = U_2^*$. Then the integrals in $\text{Re}\left\{e^{2i\nu t} \int_0^{2\pi} V_1(\phi)^2 d\phi + e^{-2i\nu t} \int_0^{2\pi} V_2(\phi)^2 d\phi\right\}$ just integrate twice around the origin in the complex plane and would yield an amplitude of $B=0$. This is not the case since A_0 and A do not commute.

So combined, we have:

$$\sigma^2 = e^{-\frac{1}{8}\epsilon t}(W + \cos(2\nu t + \Phi_0)B), \quad (7)$$

and with a term-wise square root,

$$\sigma = \begin{pmatrix} \sigma_{mn} \\ \sigma_{mc} \\ \sigma_{pc} \\ \sigma_{pn} \end{pmatrix} = e^{-\frac{1}{4}\epsilon t} \sqrt{W + \cos(2\nu t + \Phi_0)B}. \quad (8)$$

B Verification of theory

We may simulate a cellular system with $\nu = \frac{2\pi}{22}$, $r = 5$, $b = 10$, $V = 0.5$, $N_c = 150$. Additionally, set K such that $\lambda = \nu i$ and α such that $p_n^0 = 500$ is the critical value of nucleus proteins. For initial phases, we take ϕ_i randomly and uniformly sampled, and the distribution is as follows:

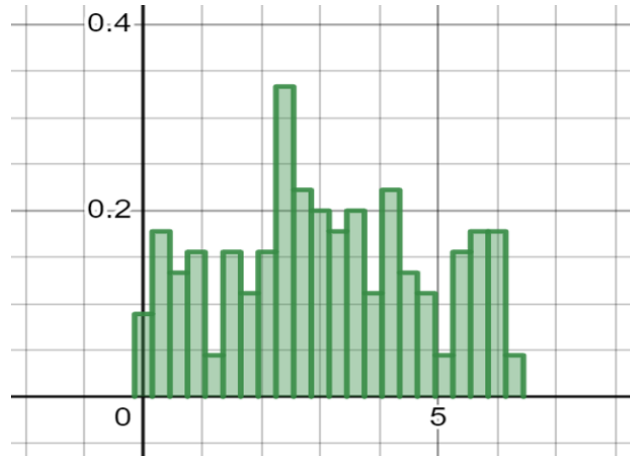


Figure 18: Distribution histogram of $\phi^i \in [0, 2\pi]$ for 150 cells with bin-size 0.3.

We set $\epsilon = \frac{2}{22}$, for the first 500 hours elapsed we obtain the results as seen in figure 19-22. From figure 22 we see that the theoretical result

$$\sigma_{pn} = e^{-\frac{1}{4}\epsilon t} \sqrt{W + \sin(2\nu t)B}$$

roughly bounds the simulated result for $W = 35000$ and $B = 10000$. These values are taken empirically, but also can be calculated from initial conditions from the formulae given, $W = 35000$ corresponds to an initial standard deviation of 187. We see that as σ_{pn} decreases toward 0, its fluctuation frequency goes from ν to 2ν . The discrepancies we see between the theory and the simulations are small, and can potentially be explained by the linear approximation we have applied to the non-linear term governing mRNA transcription.

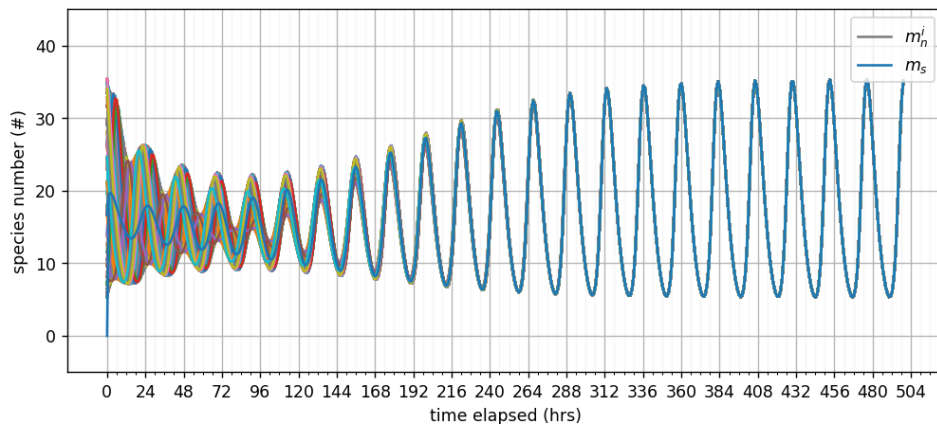


Figure 19: m_n^i vs t

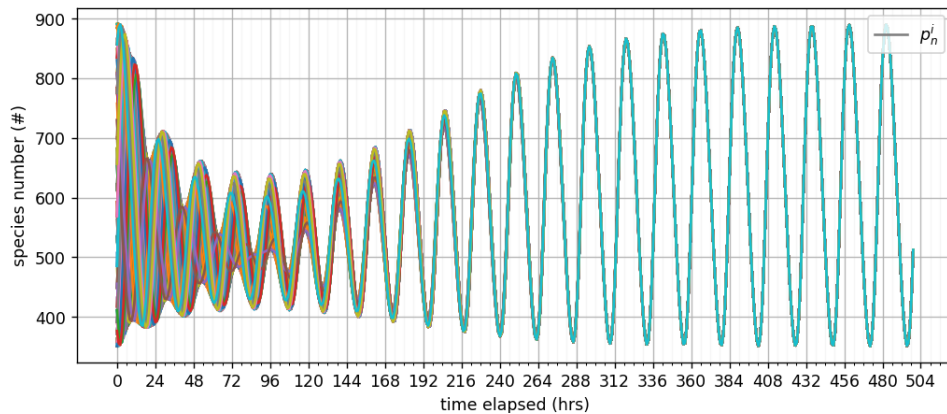


Figure 20: p_n^i vs t

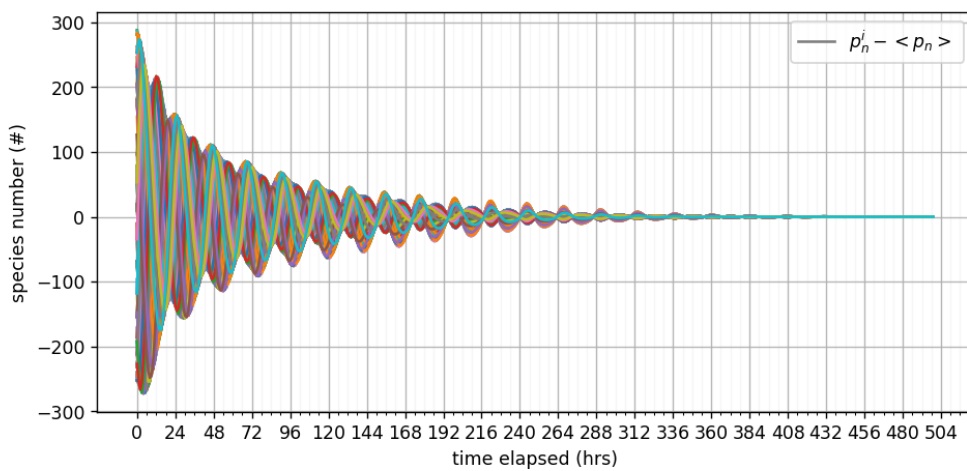


Figure 21: $p_n^i - \langle p_n \rangle$ vs t

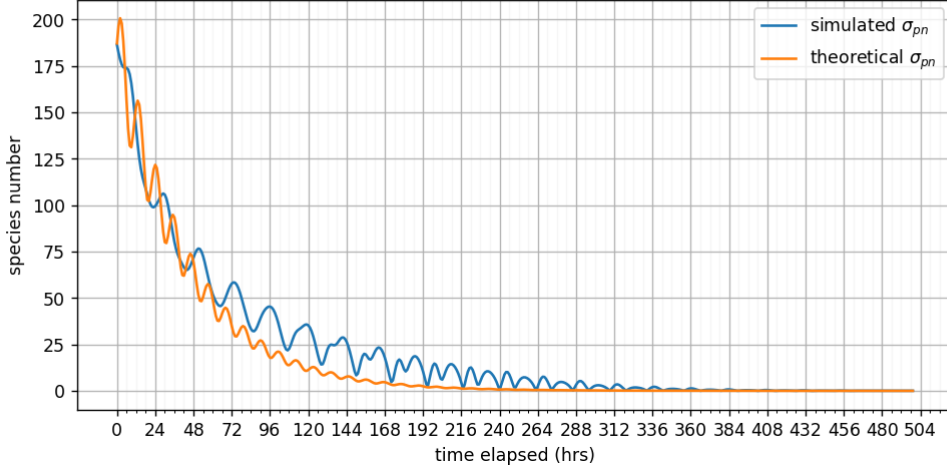


Figure 22: σ_{pn} vs t (blue), $e^{-\frac{1}{4}\epsilon t} \sqrt{W + \cos(2\nu t + \Phi_0)B}$ vs t (orange), with $W = 35000$, $B = 10000$ chosen to satisfy initial standard deviation and fluctuation range.

We may also verify the theory against initial parameters $\epsilon = \frac{3}{22}$, $\nu = \frac{2\pi}{24}$, $r = 5$, $b = 9$, $V = 0.5$, $N_c = 150$, the results are as seen in figure 23-25. From figure 25 we can see that with the increased ϵ , there is a better agreement between the theoretical prediction and the measured results, again with constants $W = 35000$ and $B = 10000$. Notably, the local fluctuations in the simulated result are of frequencies 2ν , and its phase aligns with that of the theoretical σ_{pn} .

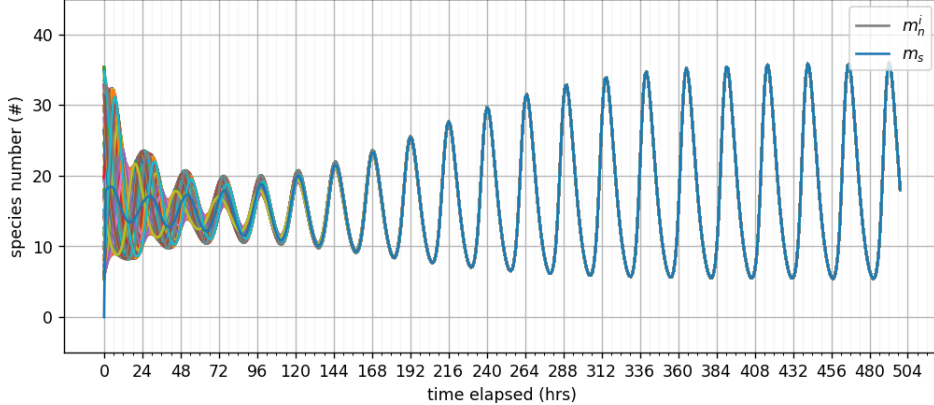


Figure 23: m_n^i vs t

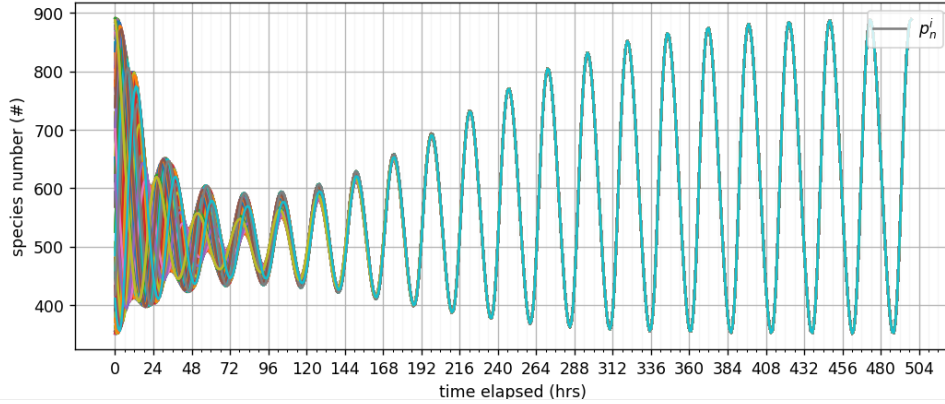


Figure 24: p_n^i vs t

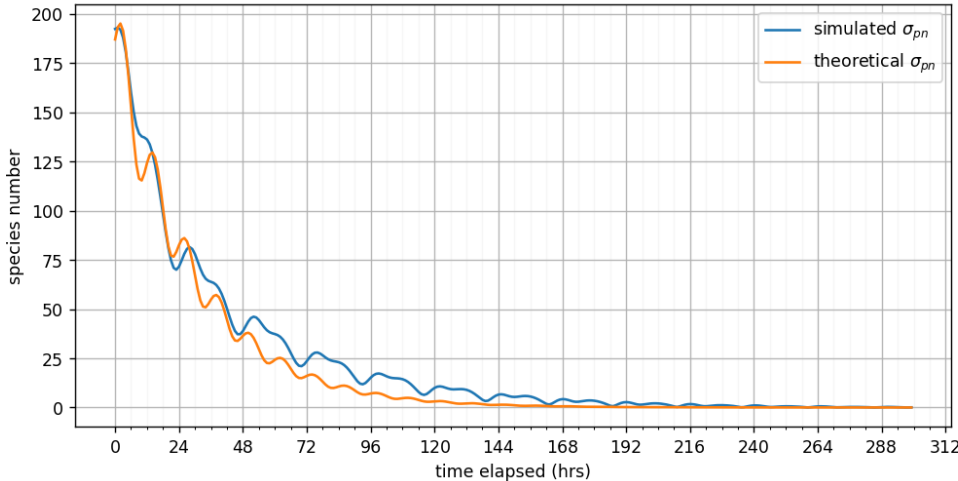


Figure 25: σ_{pn} vs t (blue), $e^{-\frac{1}{4}\epsilon t} \sqrt{W + \cos(2\nu t + \Phi_0)} B$ vs t (orange), with $W = 35000$, $B = 10000$ chosen to fit initial conditions.

References

- [1] Guanyu Wang, Charles S. Peskin, *Entrainment of a cellular circadian oscillator by light in the presence of molecular noise* (2018), Phys. Rev. E 97, 062416, <https://journals.aps.org/pre/pdf/10.1103/PhysRevE.97.062416>.
- [2] `scipy.integrate.solve_ivp`, https://docs.scipy.org/doc/scipy/reference/generated/scipy.integrate.solve_ivp.html#r179348322575-2.
- [3] J.R. Dormand, P.J. Prince, A family of embedded Runge-Kutta formulae, Journal of Computational and Applied Mathematics, Volume 6, Issue 1, 1980, Pages 19-26, ISSN 0377-0427, [https://doi.org/10.1016/0771-050X\(80\)90013-3](https://doi.org/10.1016/0771-050X(80)90013-3). (<https://www.sciencedirect.com/science/article/pii/0771050X80900133>)